論文 / 著書情報
Article / Book Information

Title	Recruitment and delivery of the fission yeast Rst2 transcription factor via a local genome structure counteracts repression by Tup1-family corepressors
Authors	Ryuta Asada, Miki Umeda, Akira Adachi, Satoshi Senmatsu, Takuya Abe, Hiroshi Iwasaki, Kunihiro Ohta, Charles S. Hoffman, Kouji Hirota
Citation	Nucleic Acids Research, Vol. 45, No. 16, pp. 9361-9371
Pub. date	2017, 9
URL	http://www.scopus.com/inward/record.url?eid=2-s2.0-85031931694&partnerID=MN8TOARS
Note	This article has been accepted for publication in Nucleic Acids Research Published by Oxford University Press.
Creative Commons	See next page.

Published online 27 June 2017

Nucleic Acids Research, 2017, Vol. 45, No. 16 ***9361–9371***
doi: 10.1093/nar/gkx555

Recruitment and delivery of the fission yeast Rst2 transcription factor via a local genome structure counteracts repression by Tup1-family corepressors

Ryuta Asada[1], Miki Umeda[1], Akira Adachi[1], Satoshi Senmatsu[1], Takuya Abe[1], Hiroshi Iwasaki[2], Kunihiro Ohta[3,4], Charles S. Hoffman[5] and Kouji Hirota[1,*]

[1]Department of Chemistry, Graduate School of Science and Engineering, Tokyo Metropolitan University, Minamiosawa 1-1, Hachioji-shi, Tokyo 192-0397, Japan, [2]Cell Biology Unit, Institute of Innovative Research, Tokyo Institute of Technology M6-11, 2-12-1 Ookayama, Meguro-ku, Tokyo 152-8550, Japan, [3]Department of Life Sciences, The University of Tokyo, Meguro-ku, Tokyo 153-8902, Japan, [4]Universal Biology Institute, The University of Tokyo, Bunkyo-ku, Tokyo 113-0033, Japan and [5]Biology Department, Boston College, Chestnut Hill, MA 02467, USA

Received March 16, 2017; Revised June 05, 2017; Editorial Decision June 13, 2017; Accepted June 14, 2017

ABSTRACT

Transcription factors (TFs) determine the transcription activity of target genes and play a central role in controlling the transcription in response to various environmental stresses. Three dimensional genome structures such as local loops play a fundamental role in the regulation of transcription, although the link between such structures and the regulation of TF binding to *cis*-regulatory elements remains to be elucidated. Here, we show that during transcriptional activation of the fission yeast *fbp1* gene, binding of Rst2 (a critical C_2H_2 zinc-finger TF) is mediated by a local loop structure. During *fbp1* activation, Rst2 is first recruited to upstream-activating sequence 1 (UAS1), then it subsequently binds to UAS2 (a critical *cis*-regulatory site located approximately 600 base pairs downstream of UAS1) through a loop structure that brings UAS1 and UAS2 into spatially close proximity. Tup11/12 (the Tup-family corepressors) suppress direct binding of Rst2 to UAS2, but this suppression is counteracted by the recruitment of Rst2 at UAS1 and following delivery to UAS2 through a loop structure. These data demonstrate a previously unappreciated mechanism for the recruitment and expansion of TF-DNA interactions within a promoter mediated by local three-dimensional genome structures and for timely TF-binding via counteractive regulation by the Tup-family corepressors.

INTRODUCTION

Precise transcriptional regulation is essential for effective responses to cellular stress and the determination of cell fate. Transcription factors (TFs) play a central role in the regulation of transcriptional networks (1). TFs determine which genes to activate or repress by recognizing and binding to their specific DNA motifs in the promoter or enhancer region of the target genes. The regulation of TF-binding is thus critical for transcription (2,3). How and when TFs choose from among the numerous binding candidates in genome DNA remains unknown.

Chromatin configuration, including nucleosome positioning, is an important determinant for TF-binding. Recent genome-wide research on TF-binding and chromatin accessibility has shown that many TFs bind to open chromatin regions that are devoid of positioned nucleosomes (4,5). Other TFs, known as 'pioneer TFs,' bind to their target sites in silent chromatin through direct binding to the nucleosomal target-DNA motif. These pioneer TFs play a role in the regulation of development and epigenetic reprogramming (6–9). Pioneer-TF-binding induces chromatin remodeling, allowing the formation of an open chromatin configuration and thereby enabling newly arrived TFs to access their binding sites (10,11). The local chromatin configuration is then further regulated by individual TFs, governing TF-binding specificity. DNA methylation is also involved in the regulation of TF-binding (12,13). For example, in murine stem cells, binding of the TF NRF1 is inhibited by DNA methylation. This inhibition is counteracted by DNA demethylation, which is mediated by other TFs, including CTCF (14). Thus, local chromatin configurations as well as epigenetic histone and DNA modifications play roles in the regulation of TF-binding specificity.

Recent studies have demonstrated that, in addition to epigenetic regulation, the three-dimensional regulation of the genome structure is important for long- and short-range gene expression. Loop structures, referred to as 'gene loops,' in which the gene promoter and terminator regions

*To whom correspondence should be addressed. Tel: +81 42 677 2542; Fax: +81 42 677 2542; Email: khirota@tmu.ac.jp

are juxtaposed, have been detected in yeast and human genes, particularly in local genomic regions (15–17). The formation of a gene loop depends on transcription, and the three-dimensional regulation of the genome structure is required for both transcriptional memory and directionality (18,19). This structure also participates in chromatin-remodeler targeting and transcriptional co-regulation in yeast and human cells (20,21). These studies suggest that three-dimensional regulation of the genome structure plays a fundamental role in the regulation of transcription. However, the mechanisms that regulate TF-binding by this structure remain largely unknown.

In fission yeast *Schizosaccharomyces pombe,* transcription of *fbp1*, which encodes fructose-1,6-bisphosphatase, is robustly induced by glucose starvation and, conversely, repressed in glucose-rich conditions (22). Transcription of *fbp1* is regulated by several TFs via the local chromatin configuration (23–27). In response to glucose starvation, chromatin configuration in the *fbp1* promoter region is progressively converted to an open state, as several species of long noncoding RNAs called mlonRNAs are transcribed (25,28). This process is required for subsequent TF-binding (25,28). Moreover, the Tup-family corepressors (Tup11 and Tup12) and three types of TF (CREB/ATF TF Atf1, the CBF/NF-Y TF Php2/5 complex and the C_2H_2 zinc-finger TF Rst2) play essential roles in the regulation of *fbp1* transcription (23,26,27,29,30). The binding sites for Atf1 and Rst2 in the *fbp1* promoter region have been defined as upstream activation sequences (UAS) 1 and UAS2, respectively (27). UAS1 contains the conserved cAMP-response element, while UAS2 contains the stress-response element (27). These sites are located 636 bp apart from each other in the upstream from the *fbp1* promoter region (Figure 1A). We previously demonstrated that both Php2 and Tup11/12 are distributed throughout the *fbp1* upstream regulatory region with peaks at UAS1 and UAS2 (29,30). Tup11 and Tup12 repress *fbp1* transcription by repressing chromatin remodeling around TF-binding sites and transcription-start sites, and by repressing transcription-apparatus binding (29). The transcriptional repression is antagonized by the three TFs required for the regulation of *fbp1* transcription and these antagonistic regulations are required for proper stress specific activation of *fbp1* transcription and for precise selection of the transcription start sites (23,29). However, how these TFs are recruited and bound to the *fbp1* promoter in a timely fashion to gain rigorous regulation of *fbp1* transcription remains largely unknown.

In this research, we demonstrate that binding of the Rst2 TF is tightly regulated through the local three-dimensional genomic structure. During glucose starvation, Rst2 is firstly recruited at UAS1 and then subsequently delivered to UAS2 through the local loop structure defined as UAS loop that brings UAS1 and UAS2 into spatially close proximity. Moreover, this loop-mediated recruitment of Rst2 counteracts Tup11/12 mediated repression of Rst2 binding to UAS2. This study demonstrates the novel regulation mechanism of the rigorous regulation of TFs binding through a local genome loop structure.

MATERIALS AND METHODS

Fission yeast strains, genetic methods and cell culture

The *S. pombe* strain used in this study is listed in Supplementary Table S1. Standard genetic procedures were carried out as described previously (31). For strain construction, sporulation agar medium was used to induce mating and sporulation, followed by tetrad dissection. Transformation was carried out using the lithium acetate method as described previously (32). To select kanamycin-resistant or uracil-auxotrophic colonies, culture suspensions were inoculated onto plates containing yeast extract (YE) and 2% glucose, incubated for 16 h, then replica-plated onto YE plates containing 100 μg/ml G-418 sulfate (Wako) or onto SD plates containing 100 μg/ml uracil and 1 mg/ml of 5-FOA (Wako), respectively. Cell culture for glucose-rich or glucose-starved was performed using yeast-extract-repression (YER) medium containing 6% glucose and yeast extract derepression (YED) medium containing 0.1% glucose and 3% glycerol.

Construction of UAS1-, UAS2- and TATA box-mutated strains

The genome sequence around UAS1, UAS2 and TATA box in the *fbp1* promoter region was amplified using primers p5 and p6 (Supplemental Table S2) and cloned into TOPO Blunt vector (Invitrogen). A *ura4*$^+$ selection cassette was inserted at the HpaI site between UAS1 and UAS2. The resultant plasmid was digested with NdeI, and transformed to gain *ura4* inserted strain at *fbp1* promoter region. Site-directed mutagenesis of UAS1 and UAS2 were performed using primers p7 and p8 and primers P9 and P10, respectively, using the method previously described (33) (Supplemental Table S2). The underlined bases in the sequence presented in Supplementary Table S2 indicate mutated sites. These mutations diminish *fbp1* transcription as well as TF-binding activity (27). In the case of the TATA box mutation, the TATA sequence of *fbp1* mRNA (34) is converted to a BamHI site as described above using primers p11 and p12 (Supplementary Table S2). The mutated plasmid was digested with NdeI and transformed into the *ura4*-inserted strain, and cells carrying the mutated UAS1, UAS2 or TATA box were selected by 5-FOA. Introduction of mutations was confirmed by sequencing.

Construction of genome-replacement strains upstream from UAS1

For the construction of sequence-replacement alleles, each 45 bp sequence upstream from UAS1, –1304 to –1260, –1259 to –1215 and –1214 to –1170 (relative to first A of the ORF) was replaced by a 45 bp sequence from the *act1* ORF region (+436 to +480). The construction of plasmids for replacement of UAS1 upstream regions and strains was performed as described above using primer pairs p13–p14, p15–p16 and p17–p18 for the regions a, b and c, respectively (Figure 5), using the method described above (Supplementary Table S2). Replacement was confirmed by sequencing. In region b (Supplementary Figure S2), 10 bp sequences –1259 to –1250, –1249 to –1240, –1239 to –1230

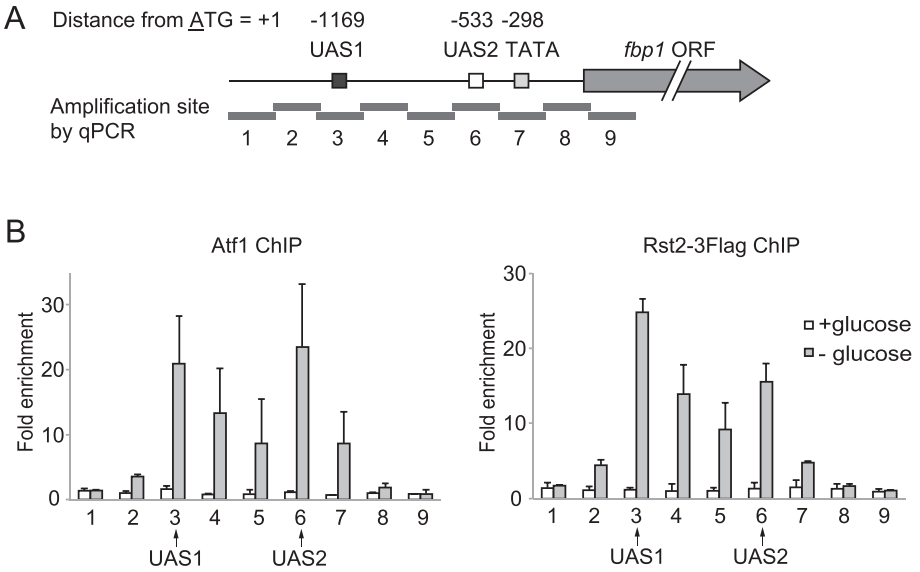

Figure 1. Atf1 and Rst2 distribute in the *fbp1* promoter region with two peaks at UAS1 and UAS2. (**A**) Schematic representation of *cis*-regulatory elements in the *fbp1* promoter region and amplification sites (determined by ChIP-qPCR) used in this study. The gray arrow represents *fbp1* ORF; the boxes represent UAS1, UAS2 and the TATA box. The position of each element is indicated as the distance from A of the first ATG in the *fbp1* ORF. The gray bars represent nine segments across the *fbp1* promoter region (detected by ChIP-qPCR). Segments 3 and 6 contain UAS1 and UAS2, respectively. (**B**) Distribution of Atf1 and Rst2 in the *fbp1* promoter region was determined by ChIP analysis. Cells were cultured in YER (+glucose) and then transferred to YED medium and cultured for 120 min (–glucose). qPCR was performed using primer pairs to detect each segment indicated in (A). The ChIP signal in the *prp3* ORF was used for normalization. Error bars represent the standard deviation from three independent experiments.

and –1229 to –1215 in the *fbp1* promoter region were replaced by *act1* ORF regions +436 to +445, +446 to +455, +456 to +465 and +466 to +480, respectively. These plasmid constructions were performed using a Primestar Max mutagenesis kit (Takara) and primer pairs p19–p20, p21–p22, p23–p24 and p25–p26 for replacement of regions i, ii, iii and iv, respectively (Supplementary Figure S2; Table S2). For the construction of the region-b translocation allele, the adjacent UAS2 sequence (–584 to –540) was replaced by the region-b sequence (–1259 to –1215). The construction of this plasmid was performed as described above using primers p27–p28 and the plasmid for replacement of region-b as template (Supplementary Table S2).

Construction of Rst2-Gal4-GBD strains

For the expression of the Gal4-GBD fusion protein, we replaced the GFP tag gene in the int2 vector (32) with the *GAL4-gbd* gene encoding N-terminus Gal4 DNA binding domain of *S. cerevisiae* (1–93 amino acid). To construct the Rst2-Gal4-GBD strain, we followed the standard integration method using the vector described above. The adjacent UAS2 sequence (–594 to –540) was replaced by the 3xGal4 binding site as described above using primer pair p29-p30 (Supplementary Table S2).

Northern blot and chromatin analysis

Northern blot and chromatin analysis were performed as described previously (30).

ChIP-qPCR

Chromatin immunoprecipitation coupled with quantitative PCR (ChIP-qPCR) was performed as described previously (29) using anti-Atf1 (abcam ab18123), Anti-DYKDDDDK (Wako 018–22383) and anti-H3 (abcam ab1791) antibody. Sequences of the primer sets (fbp1–1∼fbp1–9 and prp3 F, R) are indicated in Supplementary Table S2.

Chromosome-conformation capture

Chromosome-conformation capture (3C) analysis was performed as described previously (35), with slight modifications as briefly described below. Cells were cultured to 2.0 $\times$ 10^7/ml in 50 ml and crosslinked with 1% formaldehyde for 15 min at room temperature. The reaction was quenched by the addition of glycine to 0.125 M and incubated for 5 min at room temperature. After centrifugation, cells were washed in ice-cold TBS containing 1% triton X-100, then in ice-cold TBS without triton X-100. The cells were suspended in 1 ml of FA lysis buffer (50 mM HEPES–KOH pH 7.9, 140 mM NaCl, 1 mM EDTA, 1% Triton X-100, 0.1% sodium deoxycholate) containing proteinase inhibitor cocktail (Roche) and transferred to two 2 ml tubes containing 0.6 ml glass beads (Yasuikikai). After disruption using a bead shocker (Yasuikikai), pellets were collected by centrifugation and washed in 0.5 ml FA lysis buffer. The washed pellets were resuspended with 0.5 ml of 10 mM Tris–HCl (pH 7.5) and divided into 50 μl aliquots. 0.5 μl of 10% SDS was added and the sample was incubated for 15 min at 65°C. After incubation with 1% Triton X-100 for 30 min at 37°C, the chromatin DNA was digested by 50 U HhaI (NEB) for 5 h at 37°C and further digested with another 50 U HhaI overnight. The restriction enzyme was inacti-

vated by adding SDS to 1% and incubating for 20 min at 65°C. SDS was sequestered by incubation with 1% Triton X-100 for 30 min at 37°C. The DNA was diluted to a final volume of 700 μl by adding 2 × buffer (132 mM Tris–HCl pH 7.6, 20 mM $MgCl_2$, 2 mM DTT, 2mM ATP, 15% PEG6000) and H_2O and then ligated overnight at 16°C using a Quick ligation kit (NEB). The RNA was digested by adding 20 μg RNaseA (Nakalai). The crosslinks were reversed by overnight incubation at 65°C with 100 μg of Proteinase K (Wako) and 0.1% SDS. The DNA was purified by phenol chloroform extraction and ethanol precipitation. Because the background signal is high during 3C detection of interactions in local genomic regions, we measured interactions within a housekeeping gene, *prp3,* as an internal control to avoid experimental artifacts caused by differences in crosslinking efficiency (36). 3C PCR was performed using Taq HS polymerase (Takara) and Thermal Cycler Dice TP600 (Takara). The primers used were p1–p2 for the *fbp1* locus, and p3–p4 for the *prp3* locus. The sequence is listed in Supplementary Table S1. 20 μl PCR products were run on 2% agarose gel and band intensity was quantified using a multi gauge (FUJIFILM).

RESULTS

Distribution of TF-binding at *fbp1* upstream region

We examined the binding distribution of Atf1 and Rst2 in the *fbp1* upstream regulatory region using chromatin-immunoprecipitation (ChIP) analysis. We found that Atf1 and Rst2 binding exhibited two peaks at UAS1 and UAS2, respectively (Figure 1A and B). This is totally unexpected because Atf1 and Rst2 are expected to bind only at UAS1 and UAS2, respectively (27). Moreover, their binding pattern is very similar to that of Tup11/12 and Php2, previously reported (29,30). These data led us to hypothesize that TF-binding is mediated by the formation of local genome loop structures, wherein UAS1 and UAS2 are placed in close proximity, since, as previously demonstrated, proteins binding to one site can be detected (via ChIP analysis) on the other site (16).

Formation of a UAS loop at *fbp1* upstream region

To examine the possibility that a local loop forms in the *fbp1* upstream region, we used chromosome-conformation capture (3C) technology as described in materials and methods. The intensity of the 3C signal between UAS1 and UAS2 increased after glucose starvation, indicating proximity, whereas the signal for interaction within the *prp3* gene (internal control) was unchanged (Figure 2A and B). To quantify the 3C signal, intensity of the bands amplified using primers corresponding to UAS1 and UAS2 or primers corresponding to inside of *prp3* gene were quantified (Figure 2A). The intensity of the 3C signal linearly increased with increasing concentrations of 3C sample (Supplementary Figure S1). The intensity of the signal between UAS1 and UAS2, normalized to that of the internal control, was significantly increased at 60 and 120 min after glucose starvation (Figure 2C). These results indicate that a local genome loop structure is formed between UAS1 and UAS2 in response to glucose starvation. We define this loop structure as a UAS loop and further investigated its formation. This UAS loop between UAS1 and UAS2 might not be a simple result of the transcriptional activation. This is because, while cells lacking the *fbp1* TATA box exhibited little *fbp1* activation (Figure 2D), an increase of the 3C signal after glucose starvation was still observed with only slightly later timing than that in *wild-type* cell. This suggests that *fbp1* mRNA transcription is not required for the formation of the UAS loop and that transcriptional initiation may have an only limited, if any, impact on the formation of this structure (Figure 2E and F).

Alteration to an open configuration is a prerequisite for the formation of the UAS loop

Since chromatin remodeling in the *fbp1* upstream region is completed by 60 min after glucose starvation (25,28), it is possible that this remodeling is a prerequisite for the formation of the UAS loop. To address this, we measured the 3C signal between UAS1 and UAS2 in chromatin remodeling deficient *snf22Δ/hrp3Δ* cells (Adachi *et al.,* in press). This mutant lacks ATP dependent chromatin remodeling factors (ADCRs), Snf22 and Hrp3 and exhibits impaired chromatin remodeling at *fbp1* upstream region (Adachi *et al. in press*). While in *wild-type* cells, we detected MNase sensitive sites reflecting open chromatin configurations around UAS1–2 and UAS2-TATA after glucose starvation, we detected little change of the MNase digestion pattern in this mutant (Supplementary Figure S2A). The change in the MNase digestion pattern during glucose starvation indicates disassembly of three nucleosomes at UAS1, UAS2 and TATA box in *wild-type* cells (Supplementary Figure S2A). Consistently, we detected disassembly of histone H3 at UAS1 and UAS2 in *wild-type* cells (Supplementary Figure S2B). In the mutant lacking two redundant chromatin remodeling factors, Snf22 and Hrp3, we observed almost no change in the 3C signal after glucose starvation (Supplementary Figure S2C and D), suggesting that a chromatin-configuration change upstream of *fbp1* is indeed a prerequisite for the formation of the UAS loop.

Disruption of the UAS loop causes aberrant binding of Rst2

We explored the factors required for the formation of the UAS loop. Because a change in chromatin configuration is required to form the UAS loop (Supplementary Figure S2), we examined the requirement for Rst2 and Php5 in this process, since, although these factors bind after changes in chromatin configuration, they play a role in *fbp1* transcriptional activation (29). After glucose starvation, the increase in 3C signal intensity was significantly smaller in *rst2Δ* and *php5Δ* cells when compared to *wild-type* cells (Figure 3A and B). Therefore, Rst2 and Php2/5 are required for the UAS loop formation between UAS1 and UAS2 in the *fbp1* transcription-activation process. We next examined the binding distribution of Atf1, Php2, and Rst2 in *rst2Δ* and *php5Δ* mutants. Atf1-binding was diminished in the *rst2Δ* cells (Figure 3C), which is consistent with our earlier report (29). In contrast, loss of Php5 leads to an increase in Atf1-binding at UAS1 and a loss of binding at UAS2 (Figure 3C).

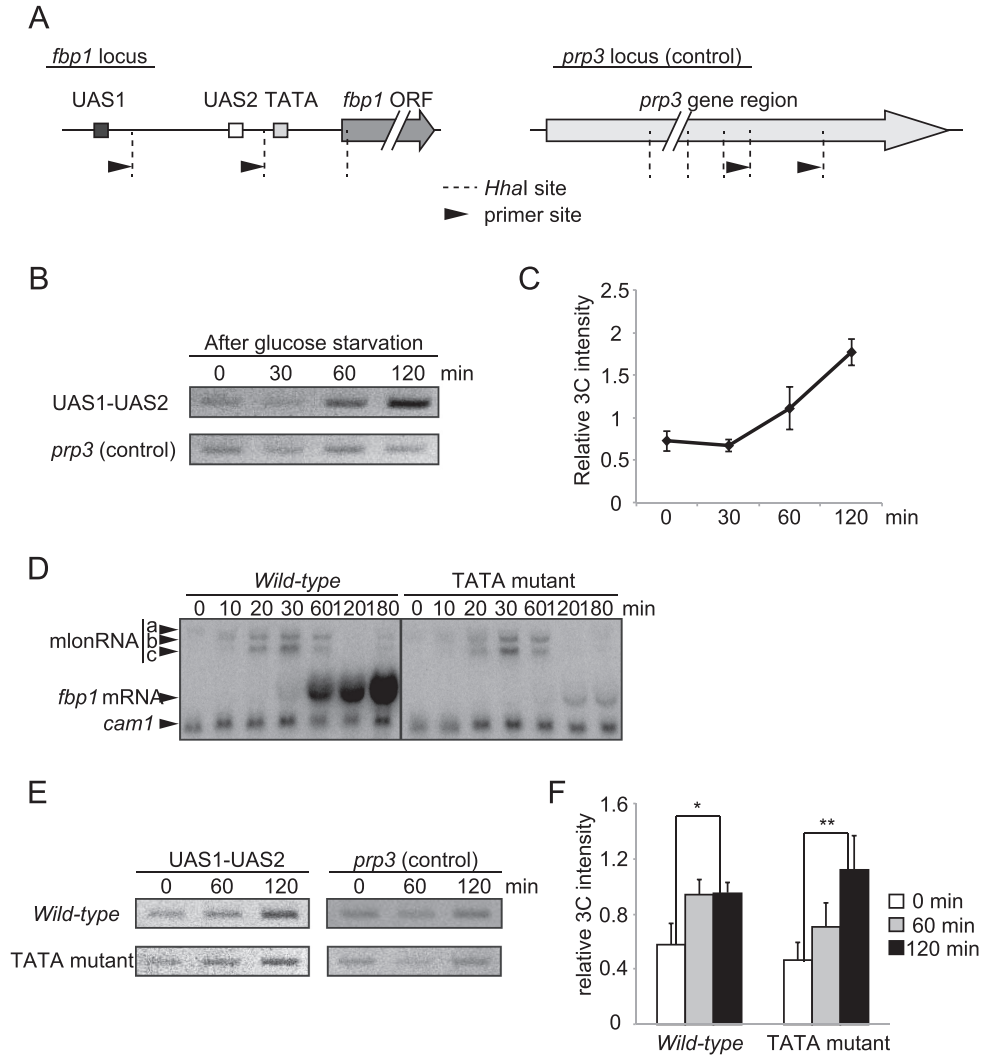

Figure 2. Formation of local genome loop in the *fbp1* upstream region after glucose starvation. (**A**) Schematic representation of restriction enzyme sites and primer sites used in 3C analysis. For the *fbp1* locus, the gray arrow represents the ORF and the boxes represent the positions of UAS1, UAS2 and the TATA box. For the control (*prp3* locus), the gray arrow represents the annotated transcription region of the *prp3* gene in Pombase (https://www.pombase.org/). The dashed lines and black arrows indicate the positions of the HhaI sites and the primer sites, respectively. The distance between the two HhaI cutting sites at the *fbp1* locus and at the *prp3* locus is 757 and 486 bp, respectively. (**B**) The association between UAS1 and UAS2 was examined by 3C analysis. *Wild-type* cells (for genes relevant to *fbp1* transcription) were cultured as in Figure 1. Cells were harvested at the indicated times. (**C**) The intensity of interactions between UAS1 and UAS2 at *fbp1* was quantified and normalized by band intensity relative to the control. Error bars show the standard deviation from three independent experiments. (**D**) The cells lacking *fbp1* TATA sequence exhibit defective *fbp1* induction after glucose starvation. Northern blot to detect *fbp1* transcripts in indicated cells. Cells were cultured as in Figure 1 and harvested at the indicated times after glucose starvation. *cam1* transcript was used as an internal control (54). (**E**) The association between UAS1 and UAS2 in the indicated cells was examined by 3C analysis as in B. (**F**) The intensity of interactions between UAS1 and UAS2 at *fbp1* was quantified as in C. Error bars show the standard deviation from three independent experiments. Statistical significance (by Student's *t*-test) is as follows: $*P < 0.05$; $**P < 0.01$.

The *php5*Δ cells also show a similar shift in the distribution of Rst2 (Figure 3D). Meanwhile, loss of Rst2 leads to a significant reduction of Php2 binding to UAS1, with no effect on UAS2 occupancy (Figure 3E). To summarize, while Atf1, Rst2, and Php2 normally associate with both UAS1 and UAS2 during *fbp1* transcriptional activation, this bimodal distribution is totally dependent on the UAS loop mediated by Rst2 and Php2/5.

Rst2 binding to the UAS1 region is independent of UAS2

The above data, which show that Rst2-binding at UAS1 is preserved in *php5*Δ cells, led us to examine the role played by UAS2 in Rst2-binding in the *fbp1* promoter region. We created UAS2-mutated cells, as previously reported (27), and analyzed Rst2-binding (ChIP analysis). In the UAS2-mutant cells, we detected Rst2-binding at UAS1 while Rst2-binding at UAS2 was significantly reduced (Figure 4A). These data suggest that Rst2 can be recruited to UAS1 independent of the UAS2 sequence. Transcription activation of *fbp1* was pronouncedly reduced in the UAS2-mutant cells, with the level of transcription defects for *fbp1* very similar in both the *rst2*Δ and the UAS2-mutant cells (Figure 4B). These results indicate that Rst2 localization at the UAS1 site is not sufficient for transcriptional activation of *fbp1* and

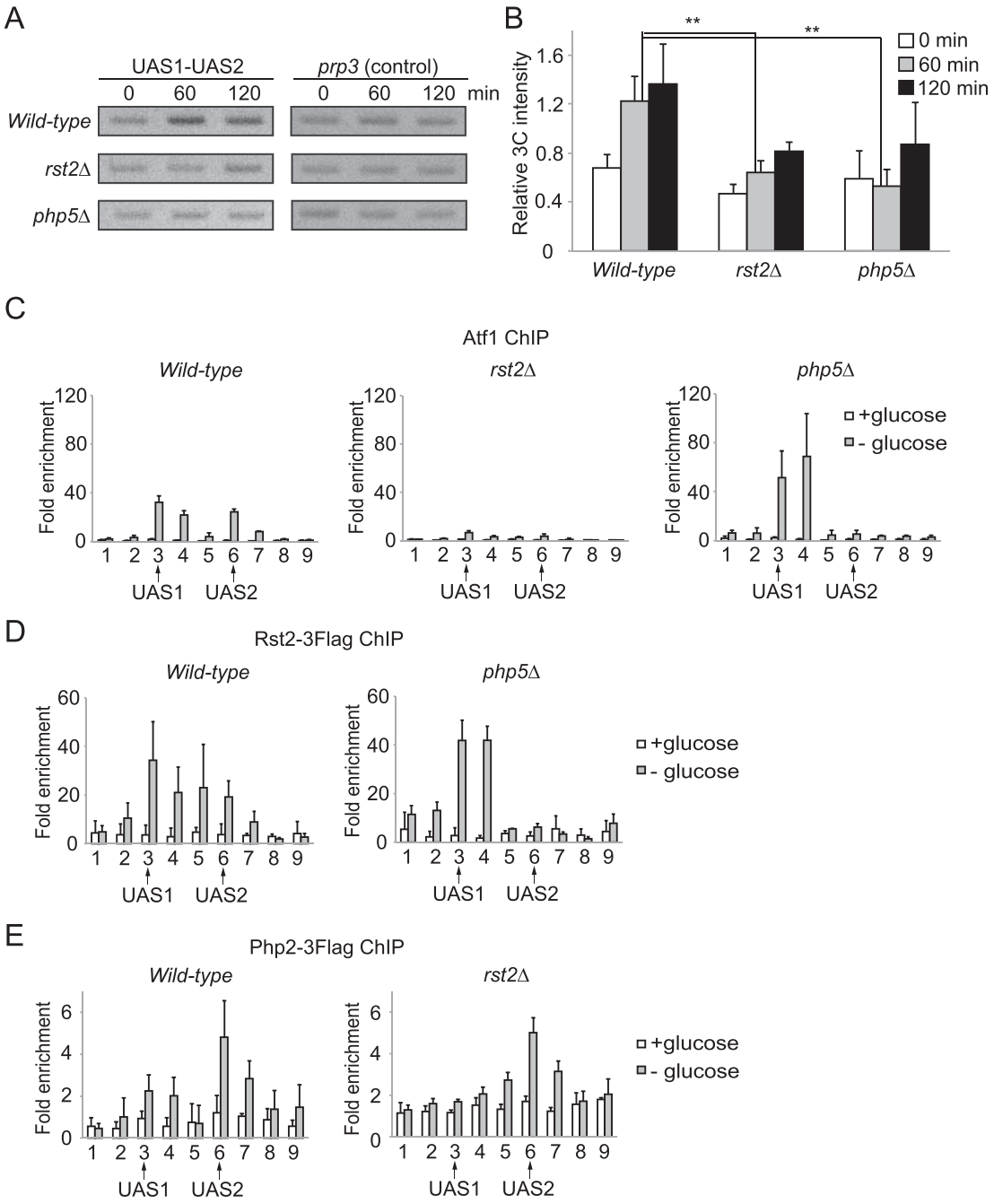

Figure 3. Formation of the UAS loop is required for the two-peak binding signature of TFs in the *fbp1* promoter region. (**A**) The association between UAS1 and UAS2 was examined by 3C analysis in *wild-type, rst2*Δ and *php5*Δ cells. (**B**) Band intensity quantitation of each strain as indicated in Figure 2C. Error bars show the standard deviation from three independent experiments. Statistical significance (by Student's *t*-test) is as follows: $^{**}P < 0.01$. (**C**–**E**) ChIP analysis to determine the distribution of Atf1, Rst2, and Php2 in *wild-type*, *rst2*Δ, and *php5*Δ cells as described in Figure 1. Error bars show the standard deviation from at least two independent experiments.

that binding at UAS2 is essential for Rst2 to carry out its function.

Identification of an Rst2-binding motif at UAS1

We next explored the newly uncovered apparent Rst2-binding motif at UAS1. Since we could not find a typical stress-response element (CCCCTC) around UAS1, we opted to replace small segments (45 bp) to detect the novel element to which Rst2 binds. As replacement downstream from UAS1 had little effect on Rst2-binding around UAS1, we examined *fbp1* transcription in mutants carrying replacements upstream from UAS1 (Figure 5A). We replaced 45 bp regions a, b or c upstream from UAS1 with *act1* ORF sequences possessing no transcription activity. Mutant cells carrying the region-b replacement exhibited a reduction in *fbp1* mRNA transcription without affecting mlonRNAs

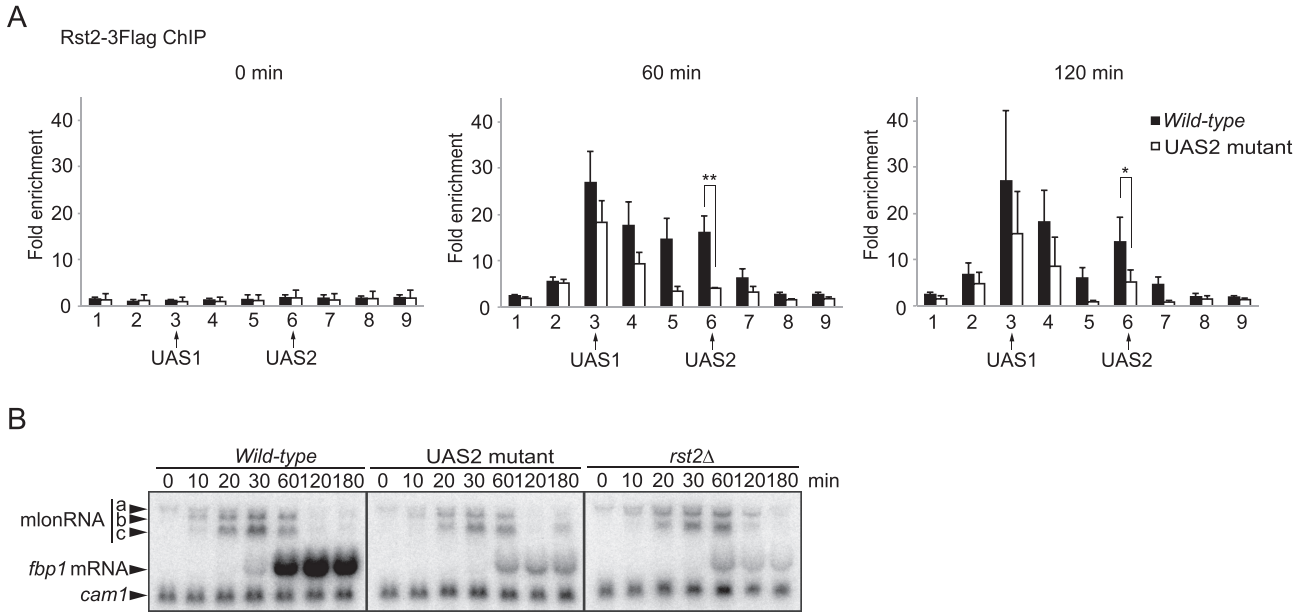

Figure 4. Rst2-binding to UAS1 is preserved in UAS2-mutant cells. (**A**) The distribution of Rst2 was examined by ChIP analysis in *wild-type* and UAS2-mutant cells. Cell culture and ChIP analysis were performed as described in Figure 1. Error bars show the standard deviation from at least two independent experiments. Statistical significance (by Student's *t*-test) is as follows: $*P < 0.05$; $**P < 0.01$. (**B**) Northern blot to detect *fbp1* transcripts in *wild-type*, UAS2 mutant and *rst2*Δ cells. Cells were cultured as in Figure 1. Cells were harvested at the indicated times after glucose starvation. *cam1* transcript was used as an internal control (54).

transcription, which is very similar to what is observed in *rst2*Δ cells (Figure 5B). Chromatin remodeling at *fbp1* upstream region was not affected in this mutant (Figure 5C), nor was it in the *rst2*Δ cells (29). To further characterize the Rst2-binding site upstream from UAS1, the 45 bp in region-b was divided into four segments, as indicated in Supplementary Figure S3A, and replaced with *act1* ORF sequences. We detected a partial but significant reduction of *fbp1* induction in mutants carrying replacements in segments i and iv (Supplementary Figure S3B). We also identified the common C/T-rich sequence in segments i and iv (Supplementary Figure S3C). To test whether the 45 bp in the region-b sequence were indeed required for Rst2-binding at UAS1, we performed a ChIP assay. We found that Rst2-binding at UAS1 was compromised in the mutant cells carrying the region-b replacement (Figure 5D). Since the region amplified by the primers for detecting UAS1 includes region-b, replacement of region-b results in the loss of Rst2 binding to this site. Unexpectedly, Rst2-binding at UAS2 was also diminished in the mutant cells carrying the region-b replacement (Figure 5D). These results suggest that the two C/T-rich motifs in region-b are primary Rst2-binding sites and that binding at UAS1 is a prerequisite for subsequent Rst2 binding at UAS2 via the formation of the UAS loop.

Rst2 switching from UAS1 to UAS2 counteracts the Tup11/12-mediated repression of Rst2-binding at UAS2

Rst2 binding at UAS2 was fully compromised in mutant cells carrying the region-b replacement, even though chromatin remodeling around UAS2 was preserved in the mutant cells (Figure 5C, D). This suggests that Rst2-binding at UAS2 is repressed by some mechanism independent of chromatin configuration. To discover this mechanism, we analyzed the Tup11/12 corepressors, because these corepressors play important roles in the regulation of *fbp1* transcription (23,29). Disruption of the Tup11/12 corepressor genes in mutant cells carrying the region-b replacement significantly restored Rst2-binding at UAS2 (Figure 5D). This result indicates that Tup11/12 repress Rst2-binding at UAS2. Taken together, these data suggest the following scenario. Rst2 is firstly recruited to UAS1 but cannot directly bind to UAS2 due to Tup11/12-mediated repression. Rst2 bound to UAS1 then associates with UAS2 through the UAS loop by counteracting the Tup11/12-mediated repression of Rst2-binding.

Forced Rst2 binding to UAS2 causes aberrant *fbp1* transcription

The above data suggest the importance of temporal regulation of binding of Rst2 to UAS2. To examine the role the temporal regulation of Rst2 binding thorough higher order genome structure, we tethered Rst2 at UAS2 using a Gal4-DNA binding domain (GBD) (Figure 6A) (37,38). Rst2-Gal4-GBD cells exhibited *fbp1* expression even under glucose rich conditions (Figure 6B), indicating that forced binding of Rst2 to UAS2 causes unregulated expression of *fbp1*.

We next examined the effect of translocation of the region-b, which is normally immediately upstream of UAS1, to a site immediately upstream of UAS2 (Figure 6C). This translocation completely rescued loss of region-b (Figure 6D). Importantly, this translocation bypassed the requirement for Php5 in *fbp1* expression (Figure 6E). These

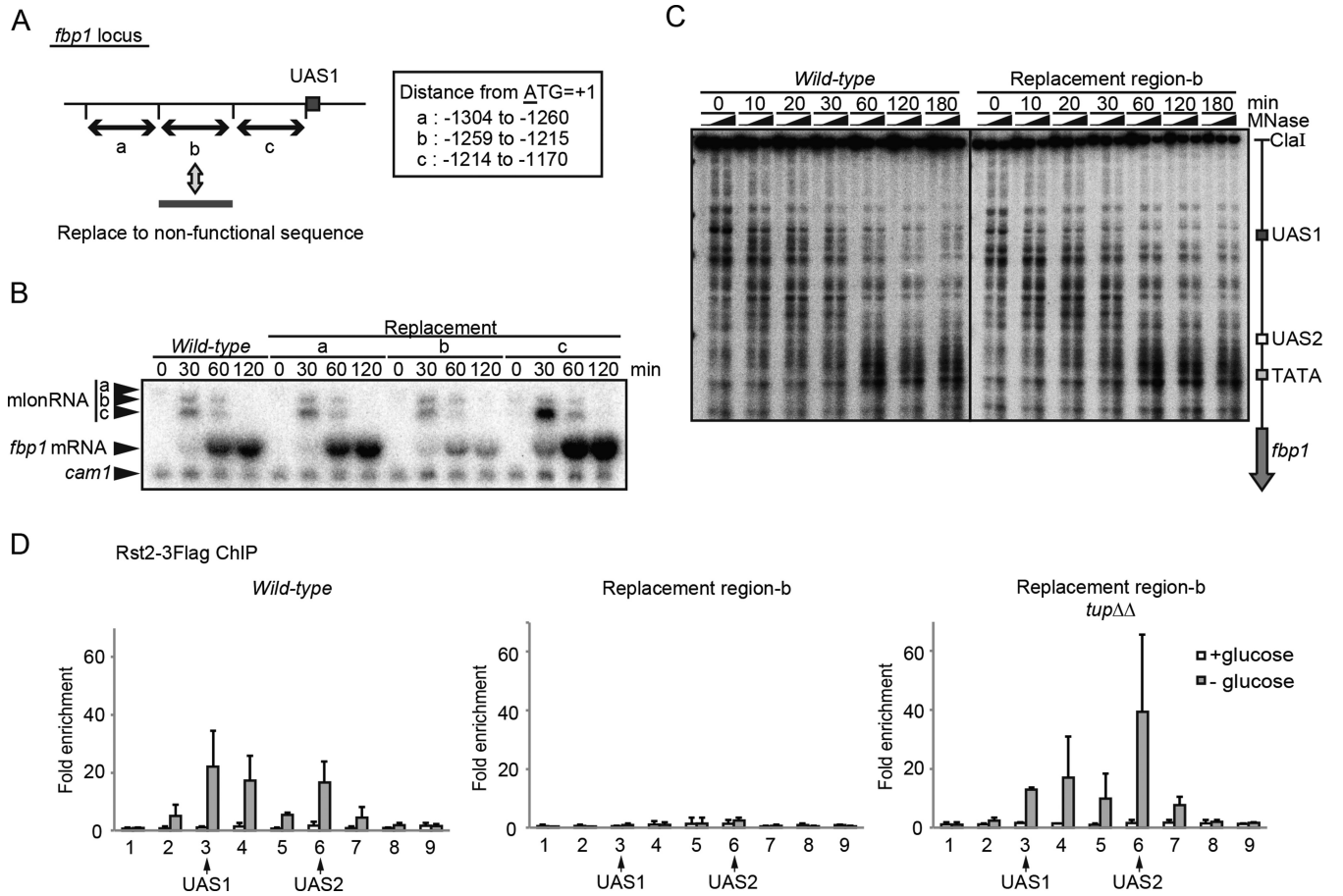

Figure 5. Rst2 switching from UAS1 counteracts Tup11/12-mediated repression of Rst2-binding at UAS2. (**A**) Schematic representation of three 45 bp regions (a, b and c) upstream from UAS1 replaced by *act1* ORF regions. (**B**) *fbp1* transcriptional activation was examined with northern blot analysis in *wild-type* cells and in cells carrying the indicated replacement region. (**C**) Chromatin analysis by MNase partial digestion of chromatin DNA upstream from *fbp1* in *wild-type* and in mutant cells carrying the replacement regions. Cells were cultured and harvested at the indicated times after glucose starvation. The isolated chromatin was partially digested by MNase with 0, 20, and 50 U/ml at 37°C for 5 min. Purified DNA was digested with ClaI and analyzed by Southern blot. (**D**) ChIP analysis of Rst2 in *wild-type* cells and in cells carrying replacement region b, and in *tup*ΔΔ cells carrying replacement region b, as described in Figure 1. Error bars show the standard deviation from at least two independent experiments.

results suggest that forced Rst2 binding to UAS2 bypasses the need for UAS loop formation. The *php5*Δ/region-b translocation cells still exhibit increased mlonRNA-c transcription and slowed transcriptional activation of *fbp1* mRNA (Figure 6E). This might be due to partial defects in evicting nucleosomes around the TATA box as previously reported (23,29).

DISCUSSION

In this study, we investigated the mechanisms that regulate TF-binding via local three-dimensional genome structure in the transcriptional activation of the fission yeast *fbp1* gene. Our study demonstrates that the formation of a local genome loop plays a critical role in regulating the binding distribution of Rst2, a C_2H_2 zinc-finger TF, in the *fbp1* promoter region during transcriptional activation. We found that the TFs required for *fbp1* induction and the Tup11/12 corepressors distribute across a wide range of the *fbp1* promoter region, exhibiting peaks at both UAS1 and UAS2 (29,30) (Figure 1). This dual-peak distribution is mediated by the local loop structure defined as a UAS loop that places UAS1 and UAS2 in close proximity. This is evidenced by the fact that an association between UAS1 and UAS2 was detected by 3C analysis after chromatin remodeling in the *fbp1* promoter region (Figure 2, Supplementary Figures S1 and S2). Furthermore, when the formation of the genome higher-order structure was diminished in *rst2*Δ or *php5*Δ cells, the two-peak distribution pattern was diminished and shifted to one peak only (Figure 3). We found that Rst2 first binds to UAS1 independent of UAS2, but this UAS1 binding is not sufficient for the transcriptional activation (Figure 4). Moreover, translocation of the Rst2 binding site near UAS1 to a position immediately upstream of UAS2 rescued the *fbp1* mRNA transcription activation defects in *php5*Δ cells, in which Rst2 binds to UAS2 independent of the UAS loop (Figure 6E). These data support the following scenario. Rst2 is initially recruited to UAS1, then it associates with UAS2 via the formation of UAS loop. This UAS loop mediated association of Rst2 antagonizes the Tup11/12-mediated blocking of Rst2-binding to UAS2.

The regulation of TF-binding may proceed in a stepwise manner. In glucose-rich conditions, closed chromatin con-

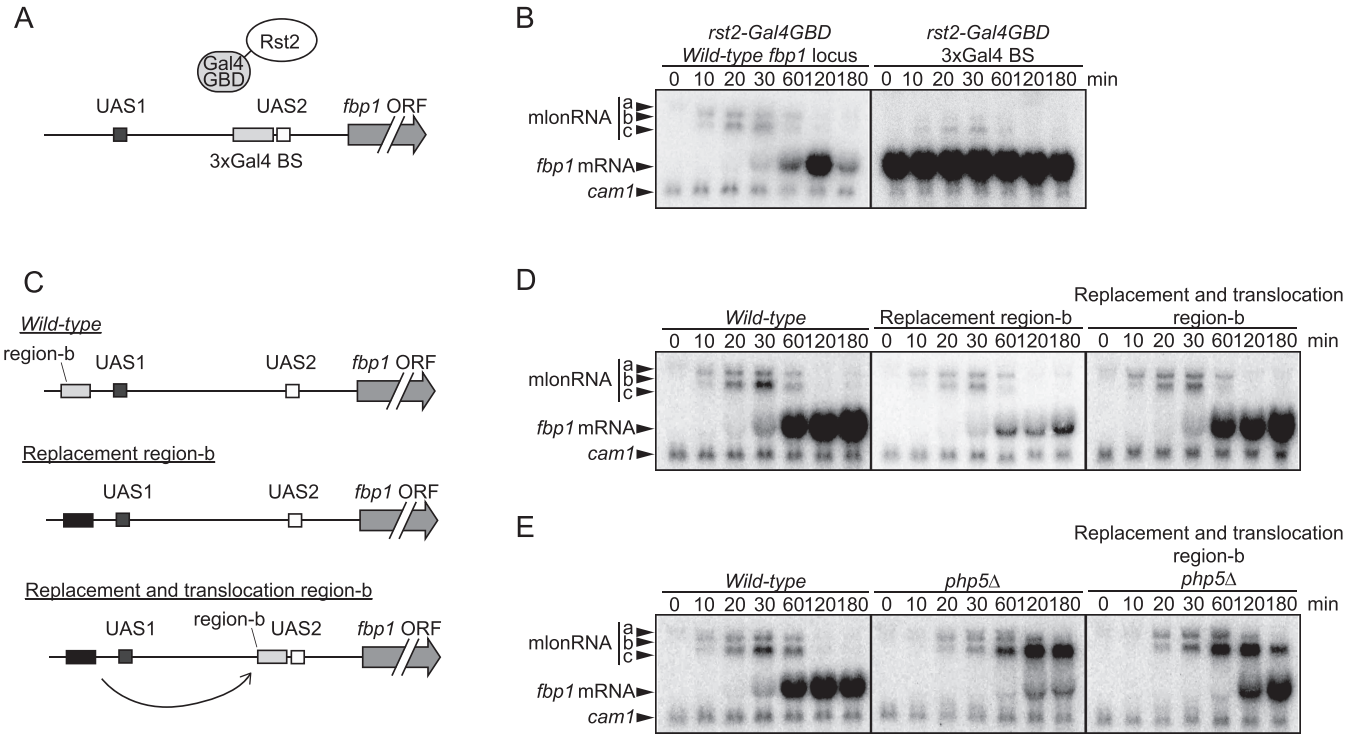

Figure 6. Forced Rst2 binding to UAS2 causes unregulated *fbp1* transcription. (**A**) Schematic representation of Rst2 tethering using Gal4-GBD. Three copies of Gal4-binding sequences (BS) were inserted at the upstream adjacent region of UAS2. Gal4-GBD was fused to the C-terminus of Rst2. The resultant fusion protein is tethered at Gal4-BS. (**B**) Gal4-GBD fusion mediated tethering of Rst2 to UAS2 causes *fbp1* activation even in the presence of glucose. *fbp1* transcriptional activation was examined with northern blot analysis in Rst2-Gal4-GBD cells. (**C**) Schematic representation of the translocation of region-b to the upstream adjacent region of UAS2. (**D**, **E**) Translocation of novel Rst2 binding site, region-b to upstream adjacent of UAS2 bypasses requirement of higher order structure formation for *fbp1* induction. Transcripts of *fbp1* were examined with northern blot analysis in indicated cells.

figurations are established in the *fbp1* upstream region (Figure 7A). This contributes to the inhibition of TF-binding. Upon glucose starvation, a cascade of mlonRNA transcriptions is initiated by Atf1-binding at UAS1, thereby inducing chromatin-remodeling around TF-binding sites, UAS1 and UAS2 (25) (Figure 7B). This chromatin configuration change enables Rst2 and Php5 to bind to their respective target sites. However, the binding of Rst2 to its binding site, UAS2, is blocked by Tup11/12, thus Rst2 binds only to the UAS1 site (Figure 7C). After Rst2 and Php5 bind at UAS1 and UAS2, respectively, the UAS loop that places UAS1 and UAS2 in close proximity is formed (Figure 7D). Rst2 bound to UAS1 then associates with UAS2, overcoming the Tup11/12-mediated block of Rst2-binding to UAS2 (Figure 7E). This UAS loop-mediated delivery of Rst2 may be important for the determination of the functional order and timing of TF-binding. Since the counteractive regulation of chromatin remodeling around the TATA box by Php5 and Tup11/12 is pivotal for the precise determination of the transcription start site (29), Rst2 might need to bind at UAS2 only after Php5 has created a suitable chromatin geometry to avoid inadequate and unregulated *fbp1* transcription.

The budding yeast Tup1 corepressor represses many stress-responsive genes (39–41), establishing repressive chromatin at target sites by recruiting histone deacetylase or by regulating the position of nucleosomes (42–44). Through the formation of repressive chromatin, *Saccharomyces cerevisiae* Tup1 and the mouse Tup1 ortholog Grg3 also inhibit the binding of TFs to their target motifs (45,46). In this study, we reveal a previously unappreciated repression mechanism by which Tup11/12 represses the binding of Rst2 to its target site without affecting chromatin structure (Figure 5C, D). Moreover, we demonstrate that this Tup11/12-mediated repression is antagonized by UAS loop-mediated delivery of Rst2. Since Tup11/12-binding at UAS2 increases during glucose starvation (29,30), this mechanism antagonizes the effect of Tup11/12 corepressors without displacing these proteins from UAS2. This Tup related repression for TFs bindings might mediate complex regulation of TFs binding to their target site and then contribute to the rigorous regulation of transcription.

We predict that TF-TF interactions in the *fbp1* upstream region might govern UAS loop formation, as previous studies have suggested that, when placed in close proximity, individual TFs carrying distinct binding motifs often interact physically and that such interactions facilitate TF-binding to target sites (47–49). Moreover, previous studies have suggested that cooperative TF-binding and formation of TF clusters in local regions play important roles in transcriptional regulation (50–53). Similarly, physical interactions between the TFs that bind at UAS1 and UAS2 might form the UAS loop at the *fbp1* locus. In fact, formation of the UAS loop is impaired in *rst2*Δ and *php5*Δ cells (Figure 3A and B). Considered alongside our current results, it seems plausible that the regulation mechanism of TF-binding via

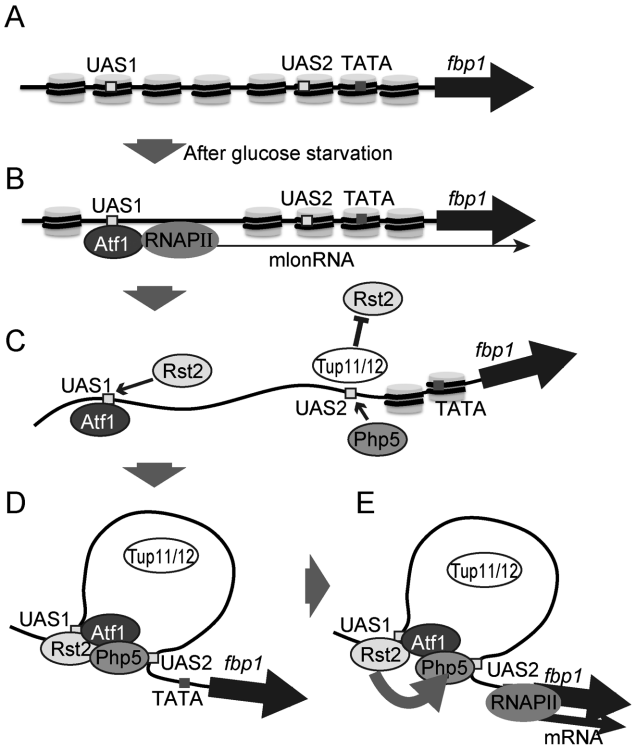

Figure 7. Model for the regulation of Rst2-binding via UAS loop formation. (**A**) In glucose-rich conditions, the *fbp1* promoter region is packaged in closed chromatin. (**B**) After glucose starvation, Atf1 activates a cascade of mlonRNA transcriptions, thereby inducing chromatin-configuration change into an open state around UAS1 and UAS2. Rst2 might stabilize Atf1 binding to UAS1. (**C**) Rst2 and Php2–5 can bind to *fbp1* UAS1 and UAS2, respectively. However, Rst2 binding to UAS2 is suppressed by the Tup11/12 corepressors. (**D**) Php2–5 binding at UAS2 induces local-chromatin remodeling into an open configuration around the TATA box, inducing the formation of a UAS loop. (**E**) Through the UAS loop, Rst2 bound to UAS1 associates with UAS2.

local genome loop formation at the *fbp1* locus might be conserved in a wide range of eukaryotic cells.

SUPPLEMENTARY DATA

Supplementary Data are available at NAR Online.

ACKNOWLEDGEMENTS

We acknowledge the Radioisotope Research Center in Tokyo Metropolitan University for support in the use of isotopes.

FUNDING

JSPS KAKENHI [25281021, 26116518, 24114509, 16K12598, 16H02957 to K.H., 15H05974, 24247033 to H.I., 26291018 to K.O. and 16J02252 to R.A.]; Takeda Science Foundation (to K.H.). Funding for open access charge: JSPS KAKENHI.
Conflict of interest statement. None declared.

REFERENCES

1. MacQuarrie,K.L., Fong,A.P., Morse,R.H. and Tapscott,S.J. (2011) Genome-wide transcription factor binding: beyond direct target regulation. *Trends Genet.*, **27**, 141–148.
2. Deplancke,B., Alpern,D. and Gardeux,V. (2016) The genetics of transcription factor DNA binding bariation. *Cell*, **166**, 538–554.
3. Slattery,M., Zhou,T., Yang,L., Dantas Machado,A.C., Gordan,R. and Rohs,R. (2014) Absence of a simple code: how transcription factors read the genome. *Trends Biochem. Sci.*, **39**, 381–399.
4. Boyle,A.P., Song,L., Lee,B.K., London,D., Keefe,D., Birney,E., Iyer,V.R., Crawford,G.E. and Furey,T.S. (2011) High-resolution genome-wide in vivo footprinting of diverse transcription factors in human cells. *Genome Res.*, **21**, 456–464.
5. Thurman,R.E., Rynes,E., Humbert,R., Vierstra,J., Maurano,M.T., Haugen,E., Sheffield,N.C., Stergachis,A.B., Wang,H., Vernot,B. *et al.* (2012) The accessible chromatin landscape of the human genome. *Nature*, **489**, 75–82.
6. Iwafuchi-Doi,M. and Zaret,K.S. (2014) Pioneer transcription factors in cell reprogramming. *Genes Dev.*, **28**, 2679–2692.
7. Morris,S.A. (2016) Direct lineage reprogramming via pioneer factors; a detour through developmental gene regulatory networks. *Development*, **143**, 2696–2705.
8. Soufi,A., Donahue,G. and Zaret,K.S. (2012) Facilitators and impediments of the pluripotency reprogramming factors' initial engagement with the genome. *Cell*, **151**, 994–1004.
9. Soufi,A., Garcia,M.F., Jaroszewicz,A., Osman,N., Pellegrini,M. and Zaret,K.S. (2015) Pioneer transcription factors target partial DNA motifs on nucleosomes to initiate reprogramming. *Cell*, **161**, 555–568.
10. Sherwood,R.I., Hashimoto,T., O'Donnell,C.W., Lewis,S., Barkal,A.A., van Hoff,J.P., Karun,V., Jaakkola,T. and Gifford,D.K. (2014) Discovery of directional and nondirectional pioneer transcription factors by modeling DNase profile magnitude and shape. *Nat. Biotechnol.*, **32**, 171–178.
11. Zaret,K.S. and Carroll,J.S. (2011) Pioneer transcription factors: establishing competence for gene expression. *Genes Dev.*, **25**, 2227–2241.
12. Blattler,A. and Farnham,P.J. (2013) Cross-talk between site-specific transcription factors and DNA methylation states. *J. Biol. Chem.*, **288**, 34287–34294.
13. Clark,S.J., Harrison,J. and Molloy,P.L. (1997) Sp1 binding is inhibited by (m)Cp(m)CpG methylation. *Gene*, **195**, 67–71.
14. Domcke,S., Bardet,A.F., Adrian Ginno,P., Hartl,D., Burger,L. and Schubeler,D. (2015) Competition between DNA methylation and transcription factors determines binding of NRF1. *Nature*, **528**, 575–579.
15. Ansari,A. and Hampsey,M. (2005) A role for the CPF 3′-end processing machinery in RNAP II-dependent gene looping. *Genes Dev.*, **19**, 2969–2978.
16. Singh,B.N. and Hampsey,M. (2007) A transcription-independent role for TFIIB in gene looping. *Mol. Cell*, **27**, 806–816.
17. Tan-Wong,S.M., French,J.D., Proudfoot,N.J. and Brown,M.A. (2008) Dynamic interactions between the promoter and terminator regions of the mammalian BRCA1 gene. *Proc. Natl. Acad. Sci. U.S.A.*, **105**, 5160–5165.
18. Tan-Wong,S.M., Wijayatilake,H.D. and Proudfoot,N.J. (2009) Gene loops function to maintain transcriptional memory through interaction with the nuclear pore complex. *Genes Dev.*, **23**, 2610–2624.
19. Tan-Wong,S.M., Zaugg,J.B., Camblong,J., Xu,Z., Zhang,D.W., Mischo,H.E., Ansari,A.Z., Luscombe,N.M., Steinmetz,L.M. and Proudfoot,N.J. (2012) Gene loops enhance transcriptional directionality. *Science*, **338**, 671–675.
20. Batista,L., Bourachot,B., Mateescu,B., Reyal,F. and Mechta-Grigoriou,F. (2016) Regulation of miR-200c/141 expression by intergenic DNA-looping and transcriptional read-through. *Nat. Commun.*, **7**, 8959.
21. Yadon,A.N., Singh,B.N., Hampsey,M. and Tsukiyama,T. (2013) DNA looping facilitates targeting of a chromatin remodeling enzyme. *Mol. Cell*, **50**, 93–103.
22. Hoffman,C.S. and Winston,F. (1991) Glucose repression of transcription of the Schizosaccharomyces pombe *fbp1* gene occurs by a cAMP signaling pathway. *Genes Dev.*, **5**, 561–571.
23. Hirota,K., Hasemi,T., Yamada,T., Mizuno,K.I., Hoffman,C.S., Shibata,T. and Ohta,K. (2004) Fission yeast global repressors

regulate the specificity of chromatin alteration in response to distinct environmental stresses. *Nucleic Acids Res.*, **32**, 855–862.
24. Hirota,K., Hoffman,C.S., Shibata,T. and Ohta,K. (2003) Fission yeast Tup1-like repressors repress chromatin remodeling at the *fbp1*$^{+}$ promoter and the ade6-M26 recombination hotspot. *Genetics*, **165**, 505–515.
25. Hirota,K., Miyoshi,T., Kugou,K., Hoffman,C.S., Shibata,T. and Ohta,K. (2008) Stepwise chromatin remodelling by a cascade of transcription initiation of non-coding RNAs. *Nature*, **456**, 130–134.
26. Janoo,R.T., Neely,L.A., Braun,B.R., Whitehall,S.K. and Hoffman,C.S. (2001) Transcriptional regulators of the Schizosaccharomyces pombe *fbp1* gene include two redundant Tup1p-like corepressors and the CCAAT binding factor activation complex. *Genetics*, **157**, 1205–1215.
27. Neely,L.A. and Hoffman,C.S. (2000) Protein kinase A and mitogen-activated protein kinase pathways antagonistically regulate fission yeast *fbp1* transcription by employing different modes of action at two upstream activation sites. *Mol. Cell. Biol.*, **20**, 6426–6434.
28. Takemata,N., Oda,A., Yamada,T., Galipon,J., Miyoshi,T., Suzuki,Y., Sugano,S., Hoffman,C.S., Hirota,K. and Ohta,K. (2016) Local potentiation of stress-responsive genes by upstream noncoding transcription. *Nucleic Acids Res.*, **44**, 5174–5189.
29. Asada,R., Takemata,N., Hoffman,C.S., Ohta,K. and Hirota,K. (2015) Antagonistic controls of chromatin and mRNA start site selection by Tup family corepressors and the CCAAT-binding factor. *Mol. Cell. Biol.*, **35**, 847–855.
30. Hirota,K., Hoffman,C.S. and Ohta,K. (2006) Reciprocal nuclear shuttling of two antagonizing Zn finger proteins modulates Tup family corepressor function to repress chromatin remodeling. *Eukaryot. Cell*, **5**, 1980–1989.
31. Gutz,H., Heslot,H., Leupold,U. and Loprieno,N. (1974) Plenum, NY, Vol. **1**, pp. 395–446.
32. Hirota,K., Tanaka,K., Watanabe,Y. and Yamamoto,M. (2001) Functional analysis of the C-terminal cytoplasmic region of the M-factor receptor in fission yeast. *Genes Cells*, **6**, 201–214.
33. Hirota,K., Tsuda,M., Mohiuddin, Tsurimoto,T., Cohen,I.S., Livneh,Z., Kobayashi,K., Narita,T., Nishihara,K., Murai,J. *et al.* (2016) In vivo evidence for translesion synthesis by the replicative DNA polymerase delta. *Nucleic Acids Res.*, **44**, 7242–7250.
34. Hoffman,C.S. and Winston,F. (1989) A transcriptionally regulated expression vector for the fission yeast Schizosaccharomyces pombe. *Gene*, **84**, 473–479.
35. El Kaderi,B., Medler,S. and Ansari,A. (2012) Analysis of interactions between genomic loci through Chromosome Conformation Capture (3C). *Curr. Protoc. Cell Biol.*, doi:10.1002/0471143030.cb2215s56.
36. Dekker,J. (2006) The three 'C' s of chromosome conformation capture: controls, controls, controls. *Nat. Methods*, **3**, 17–21.
37. Johnston,M. (1987) A model fungal gene regulatory mechanism: the GAL genes of Saccharomyces cerevisiae. *Microbiol. Rev.*, **51**, 458–476.
38. Pecina,A., Smith,K.N., Mezard,C., Murakami,H., Ohta,K. and Nicolas,A. (2002) Targeted stimulation of meiotic recombination. *Cell*, **111**, 173–184.
39. Courey,A.J. and Jia,S. (2001) Transcriptional repression: the long and the short of it. *Genes Dev.*, **15**, 2786–2796.
40. Malave,T.M. and Dent,S.Y. (2006) Transcriptional repression by Tup1-Ssn6. *Biochem. Cell Biol.*, **84**, 437–443.
41. Smith,R.L. and Johnson,A.D. (2000) Turning genes off by Ssn6-Tup1: a conserved system of transcriptional repression in eukaryotes. *Trends Biochem. Sci.*, **25**, 325–330.
42. Davie,J.K., Edmondson,D.G., Coco,C.B. and Dent,S.Y. (2003) Tup1-Ssn6 interacts with multiple class I histone deacetylases *in vivo*. *J. Biol. Chem.*, **278**, 50158–50162.
43. Zhang,Z. and Reese,J.C. (2004) Redundant mechanisms are used by Ssn6-Tup1 in repressing chromosomal gene transcription in Saccharomyces cerevisiae. *J. Biol. Chem.*, **279**, 39240–39250.
44. Zhang,Z. and Reese,J.C. (2004) Ssn6-Tup1 requires the ISW2 complex to position nucleosomes in Saccharomyces cerevisiae. *EMBO J.*, **23**, 2246–2257.
45. Buck,M.J. and Lieb,J.D. (2006) A chromatin-mediated mechanism for specification of conditional transcription factor targets. *Nat. Genet.*, **38**, 1446–1451.
46. Sekiya,T. and Zaret,K.S. (2007) Repression by Groucho/TLE/Grg proteins: genomic site recruitment generates compacted chromatin in vitro and impairs activator binding *in vivo*. *Mol. Cell*, **28**, 291–303.
47. Cheng,Q., Kazemian,M., Pham,H., Blatti,C., Celniker,S.E., Wolfe,S.A., Brodsky,M.H. and Sinha,S. (2013) Computational identification of diverse mechanisms underlying transcription factor-DNA occupancy. *PLoS Genet.*, **9**, e1003571.
48. Isakova,A., Berset,Y., Hatzimanikatis,V. and Deplancke,B. (2016) Quantification of cooperativity in heterodimer-DNA binding improves the accuracy of binding specificity models. *J. Biol. Chem.*, **291**, 10293–10306.
49. Slattery,M., Riley,T., Liu,P., Abe,N., Gomez-Alcala,P., Dror,I., Zhou,T., Rohs,R., Honig,B., Bussemaker,H.J. *et al.* (2011) Cofactor binding evokes latent differences in DNA binding specificity between Hox proteins. *Cell*, **147**, 1270–1282.
50. MacArthur,S., Li,X.Y., Li,J., Brown,J.B., Chu,H.C., Zeng,L., Grondona,B.P., Hechmer,A., Simirenko,L., Keranen,S.V. *et al.* (2009) Developmental roles of 21 Drosophila transcription factors are determined by quantitative differences in binding to an overlapping set of thousands of genomic regions. *Genome Biol.*, **10**, R80.
51. Panne,D., Maniatis,T. and Harrison,S.C. (2007) An atomic model of the interferon-beta enhanceosome. *Cell*, **129**, 1111–1123.
52. Reddy,T.E., Gertz,J., Pauli,F., Kucera,K.S., Varley,K.E., Newberry,K.M., Marinov,G.K., Mortazavi,A., Williams,B.A., Song,L. *et al.* (2012) Effects of sequence variation on differential allelic transcription factor occupancy and gene expression. *Genome Res.*, **22**, 860–869.
53. Gertz,J., Savic,D., Varley,K.E., Partridge,E.C., Safi,A., Jain,P., Cooper,G.M., Reddy,T.E., Crawford,G.E. and Myers,R.M. (2013) Distinct properties of cell-type-specific and shared transcription factor binding sites. *Mol. Cell*, **52**, 25–36.
54. Takeda,T. and Yamamoto,M. (1987) Analysis and in vivo disruption of the gene coding for calmodulin in Schizosaccharomyces pombe. *Proc. Natl. Acad. Sci. U.S.A.*, **84**, 3580–3584.